J|A|C|S
ARTICLES
Published on Web 03/01/2003

Amine- and Ether-Chelated Aryllithium Reagents—Structure and Dynamics

Hans J. Reich,* Wayne S. Goldenberg, Aaron W. Sanders, Kevin L. Jantzi, and C. Christoph Tzschucke

Contribution from the Department of Chemistry, University of Wisconsin, Madison, Wisconsin 53706

Received August 27, 2002; E-mail: reich@chem.wisc.edu

Abstract: Chelation and aggregation in phenyllithium reagents with potential 6- and 7-ring chelating amine (**2**, **3**) and 5-, 6-, and 7-ring chelating ether (**4**, **5**, **6**) ortho substituents have been examined utilizing variable temperature ^{6}Li and ^{13}C NMR spectroscopy, ^{6}Li and ^{15}N isotope labeling, and the effects of solvent additives. The 5- and 6-ring ether chelates (**4**, **5**) compete well with THF, but the 6-ring amine chelate (**2**) barely does, and 7-ring amine chelate (**3**) does not. Compared to model compounds (e.g., 2-ethylphenyllithium **7**), which are largely monomeric in THF, the chelated compounds all show enhanced dimerization (as measured by $K = [D]/[M]^2$) by factors ranging from 40 (for **6**) to more than 200 000 (for **4** and **5**). Chelation isomers are seen for the dimers of **5** and **6**, but a chelate structure could be assigned only for 2-(2-dimethylaminoethyl)phenyllithium (**2**), which has an A-type structure (both amino groups chelated to the same lithium in the dimer) based on NMR coupling in the ^{15}N, ^{6}Li labeled compound. Unlike the dimer, the monomer of **2** is not detectably chelated. With the exception of 2-(methoxymethyl)phenyllithium (**4**), which forms an open dimer (**12**) and a pentacoordinate monomer (**13**), the lithium reagents all form monomeric nonchelated adducts with PMDTA.

Chelation effects are ubiquitous in the design of organolithium reagents and interpretation of their chemistry. We have undertaken systematic studies of several classes of such reagents to establish the existence of chelation (i.e., determine the winner in the competition between external and internal solvation) and to determine the effects of the chelate ring size and chelating atom (N or O[1b,c]) on the structural,[1d] stereochemical,[1f] and chemical properties of such lithium reagents. In a previous paper, the solution structure and dynamics of a series of five-membered ring ortho amine-chelated phenyllithium derivatives (e.g., **1**) were analyzed.[1a,1h] We report here full details on the solution behavior of aryllithiums **2** and **3** with potentially chelated six- and seven-membered ring amines, as well as the analogous series of reagents with pendant ether linkages at the ortho position which could form 5, 6, and seven-membered ether chelates (**4**−**6**).[1g]

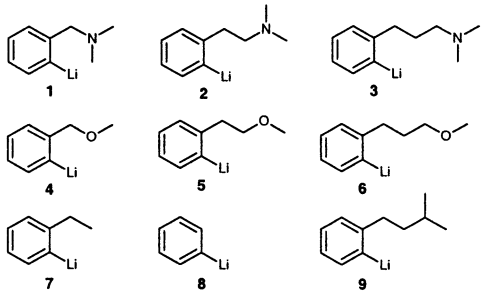

There is a substantial literature on the chemistry of chelated organolithium reagents, beginning with early reports by Hauser on the chelation-assisted ortho metalation of *N*,*N*-dimethylbenzylamine to form **1**[2] and followed by numerous studies of assisted metalation of aryl, vinyl and alkyl protons.[3a,c,43,4] Chelation effects are widely used in organolithium chemistry as design elements to facilitate metalations and increase structural rigidity,[3a,4−6] as well as to provide rationales for stereochemical, regiochemical and reactivity effects. Although

(1) (a) Reich, H. J.; Gudmundsson, B. Ö. *J. Am. Chem. Soc.* **1996**, *118*, 6074−6075. (b) Reich, H. J.; Kulicke, K. J. *J. Am. Chem. Soc.* **1995**, *117*, 6621−6622. (c) Reich, H. J.; Kulicke, K. J. *J. Am. Chem. Soc.* **1996**, *118*, 273−274. (d) Reich, H. J.; Sikorski, W. H.; Gudmundsson, B. Ö.; Dykstra, R. R. *J. Am. Chem. Soc.* **1998**, *120*, 4035−4036. (e) Reich, H. J.; Holladay, J. E. *J. Am. Chem. Soc.* **1995**, *117*, 8470−8471. (f) Reich, H. J.; Dykstra, R. R. *Angew. Chem., Int. Ed. Engl.* **1993**, *32*, 1469−1470. (g) Some of these results were reported in a preliminary communication: Reich, H, J.; Goldenberg, W. S.; Sanders, A. W.; Tzschucke, C. C. *Org. Lett.* **2001**, *3*, 33−36. (h) Reich, H. J.; Goldenberg, W. S.; Gudmundsson, B. Ö.; Sanders, A. W.; Kulicke, K. J.; Simon, K.; Guzei, I. A. *J. Am. Chem. Soc.* **2001**, *123*, 8067−8079. (i) Reich, H. J.; Green, D. P.; Medina, M. A.; Goldenberg, W. S.; Gudmundsson, B. Ö.; Dykstra, R. R.; Phillips, N. H. *J. Am. Chem. Soc.* **1998**, *120*, 7201−7210. (j) The sample temperature during the NMR experiment was measured using the tris(trimethylsilyl)methane internal ^{13}C NMR chemical shift thermometer: Sikorski, W. H.; Sanders, A. W.; Reich, H. J. *Magn. Reson. Chem.* **1998**, *36*, S118−S124. (k) DNMR simulations and integrations of overlapping peaks were performed with a version of the computer program WINDNMR (Reich, H. J. *J. Chem. Educ. Software*, **1996**, 3D, 2; http://www.chem.wisc.edu/areas/reich/plt/windnmr.htm).

(2) Jones, F. N.; Zinn, M. F.; Hauser, C. R. *J. Org. Chem.* **1963**, *28*, 663−665. Klein, K. P.; Hauser, C. R. *J. Org. Chem.* **1967**, *32*, 1479−1483.

(3) (a) Beak, P.; Snieckus, V. *Acc. Chem. Res.* **1982**, *15*, 306−312. Snieckus, V. *Chem. Rev.* **1990**, *90*, 879−933. Beak, P.; Meyers, A. I. *Acc. Chem. Res.* **1986**, *19*, 356−363. (b) Beak, P.; Kerrick, S. T.; Gallagher, D. J. *J. Am. Chem. Soc.* **1993**, *115*, 10 628−10 636. (c) Gschwend, H. W.; Roderiquez, H. R. *Org. React.* **1979**, *26*, 1−360.

recent work has provided substantial insights into the consequences of chelation,[1a−d,3b,4b,c,7a,8−10] these applications are still hampered by a lack of knowledge about the strength and even the occurrence of chelation. There is no question from single-crystal X-ray structures that organolithium reagents with pendant alkoxy and amino groups are chelated under poorly solvated or solvent-free conditions.[11] It is, however, less clear how well such chelating groups compete with commonly used ethereal solvents such as THF.[1e,14]

Results and Discussion

Syntheses. The lithium reagents were prepared by Li/Sn exchange of the appropriate *o*-trimethylstannyl compounds, typically in diethyl or dimethyl ether solution, from which most of the lithium reagents could be purified by crystallization. The bromo precursors of the tin derivatives were not used directly because of interference from lithium bromide (if *t*-BuLi was used) or 1- and 2-bromobutane (if *n*- or *sec*-BuLi was used). To facilitate NMR studies, the ^{6}Li enriched isotopomers[7d] of all compounds were prepared and the amines were synthesized in ^{15}N enriched form. The synthesis of the amines is illustrated for **2** in Scheme 1. Compound **3** was prepared analogously from 3-(2-bromophenyl)propanoic acid. The ethers **4** and **5** were prepared by straightforward methods.[15]

Scheme 1

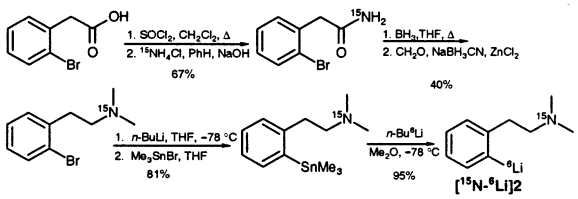

Table 1. Thermodynamic and Kinetic Data for Chelated Aryllithiums and Model Compounds

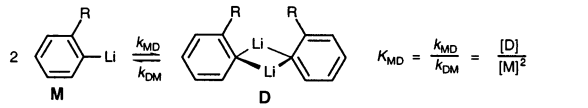

compd	R	K_{MD}/M^{-1}	ΔG° [a] (*T*/°C)	$\Delta G^{\ddagger}_{DM}$ [a] (*T*/°C)
8	−H	210	−1.5 (−128)[b]	8.3[c] (−101)[d]
	$-CH_3$	1.7	−0.2 (−135)[e]	
7	$-CH_2CH_3$	0.19	0.4 (−140)[b]	6.8[b] (−139)[b]
9	$-(CH_2)_2$-*i*Pr[f]	<0.23	≥0.6 (−125)[b]	
1	$-CH_2NMe_2$[f]	>17 000	≤−2.6 (−131)[b]	>12.5[g,h] (−36)[b]
2	$-(CH_2)_2NMe_2$	226	−1.5 (−137)[b]	9.4[k] (−107)[i]
3	$-(CH_2)_3NMe_2$	<0.23	≥0.6 (−130)[i]	
4	$-CH_2OMe$	>35 400	≤−3.0 (−127)[b]	≥9.5[g] (−80)[j]
5	$-(CH_2)_2OMe$	11 000	−2.8 (−121)[b]	10.7[k] (−83)[b]
6	$-(CH_2)_3OMe$	12	−0.7 (−141)[b]	8.8[j](−107)[i]

[a] Free energies in kcal/mol for k_{DM} and K_{DM}. ΔG° is the free energy difference between a dimer and two molecules of monomer. [b] 3:2 THF/Et_2O. [c] Ref 1i. [d] THF. [e] 4:1 THF/Et_2O. [f] Ref 1h. [g] Coalescence of the 1:2:3:2:1 quintet of the C−Li carbon. [h] The rate is bimolecular. [i] 3:2:1 THF/Me_2O/Et_2O. [j] 3:2:1 Me_2O/THF/Et_2O. [k] Exchange of monomer and dimer signals in ^{6}Li NMR spectrum.

Solution Structures. All of the lithium reagents were studied by low temperature ^{13}C, ^{6}Li, ^{7}Li, and, where appropriate, ^{31}P NMR spectroscopy in mixed solvents containing THF with dimethyl and/or diethyl ether as cosolvents to allow operation at temperatures below the freezing point of THF (−108.5 °C). The effects of cosolvents *N*,*N*,*N*′,*N*′-tetramethylethylenediamine (TMEDA), *N*,*N*,*N*′,*N*″,*N*″-pentamethyldiethylenetriamine (PMDTA) and hexamethylphosphoric triamide (HMPA[15]) were also studied, since these provided a window into the strength and nature of chelation and aggregation.

Table 1 summarizes the thermodynamic and kinetic data we have gathered for compounds **1**−**9**. Table 2 presents chemical shift and coupling information. In particular, the ^{13}C chemical shifts of the C−Li carbon provided a clear definition of the aggregation state of the lithium reagents,[15] the monomers have C-1 at ca. δ 195 and dimers at ca. δ 187. These assignments were supported by the C−Li coupling observed, a 1:1:1 triplet for the monomeric ^{6}Li enriched compounds, and a 1:2:3:2:1 quintet for the dimers. The observation of a quintet does not rule out cyclic trimers. In cases where two aggregates were present (**2**, **5**, **6**), we determined their concentration dependence to establish the molecularity.

Lithium NMR Spectra. The ^{6}Li/^{7}Li NMR spectra were also very informative in determining the solution structure. Figure 1 summarizes the ^{6}Li spectra obtained. These spectra will be discussed in more detail in the individual sections below.

Model Systems−2-Ethylphenyllithium (**7**). A principal focus of our studies is the relationship between chelation affects and the level of aggregation. To allow a distinction to be made

(4) (a) Klumpp, G. W. *Recl. Trav. Chim. Pays-Bas* **1986**, *105*, 1−21. (b) Luitjes, H.; Schakel, M.; Schmitz, R. F.; Klumpp, G. W. *Angew. Chem., Int. Ed. Engl.* **1995**, *34*, 2152−2153. (c) Schmitz, R. F.; Schakel, M.; Vos, M.; Klumpp, G. W. *Chem. Commun.* **1998**, 1099−1100. (d) Klumpp, G. W.; Geurink, P. J. A.; Spek, A. L.; Duisenberg, A. J. M. *J. Chem. Soc., Chem. Commun.* **1983**, 814−816. (e) Moene, W.; Schakel, M.; Hoogland, G. J. M.; de Kanter, F. J. J.; Klumpp, G. W.; Spek, A. L. *Tetrahedron Lett.* **1990**, *31*, 2641−2642. (f) Moene, W.; Vos, M.; de Kanter, F. J. J.; Klumpp, G. W. *J. Am. Chem. Soc.* **1989**, *111*, 3463−3465. (g) Klumpp, G. W.; Vos M.; de Kanter, F. J. J.; Slob, C.; Krabbendam, H.; Spek, A. L. *J. Am. Chem. Soc.* **1985**, *107*, 8292−8294. (h) Vos, M.; de Kanter, F. J. J.; Schakel, M.; van Eikema Hommes, N. J. R.; Klumpp, G. W. *J. Am. Chem. Soc.* **1987**, *109*, 2187−2188. (i) Geurink, P. J. A.; Klumpp, G. W. *J. Am. Chem. Soc.* **1986**, *108*, 538−539.
(5) Paquette, L. A.; Kuo, L. H.; Tae, J. *J. Org. Chem.* **1998**, *63*, 2010−2021. Smyj, R. P.; Chong, M. J. *Org. Lett.* **2000**, *3*, 2903−2906.
(6) Lamothe, S.; Chan, T. H. *Tetrahedron Lett.* **1991**, *32*, 1847−1850. Hartley, R. C.; Lamothe, S.; Chan, T. H. *Tetrahedron Lett.* **1993**, *34*, 1449−1452.
(7) (a) Fraenkel G.; Cabral J.; Lanter C.; Wang, J. *J. Org. Chem.* **1999**, *64*, 1302−1310. Fraenkel G.; Duncan J. H.; Wang J. *J. Am. Chem. Soc.* **1999**, *121*, 432−443. (b) For an insightful discussion of dynamic processes involving C−Li multiplets in monomeric aryllithium reagents, see: Fraenkel, G.; Subramanian, S.; Chow, A. *J. Am. Chem. Soc.* **1995**, *117*, 6300−6307. (c) Fraenkel, G.; Chow, A.; Winchester, W. R. *J. Am. Chem. Soc.* **1990**, *112*, 6190−6198. (d) For many organolithium reagents, especially aggregated ones, quadrupolar broadening is severe enough with ^{7}Li (92.6% natural abundance) that C−Li coupling cannot be resolved. The ^{6}Li analogues show little or no quadrupolar broadening and thus couplings are more easily seen. Fraenkel, G.; Fraenkel, A. M.; Geckle, M. J.; Schloss, F. *J. Am. Chem. Soc.* **1979**, *101*, 4745−4747.
(8) Sato, D.; Kawasaki, H.; Shimada, I.; Arata, Y.; Okamura, K.; Date, T.; Koga, K. *J. Am. Chem. Soc.* **1992**, *114*, 761−763.
(9) Arvidsson, P. I.; Hilmersson, G.; Ahlberg, P. *J. Am. Chem. Soc.* **1999**, *121*, 1883−1887.
(10) Intramolecular comparison of a 5- and 6-ring ether chelated vinyllithium reagent suggested that the 5-ring chelate is stronger. Mitchell, T. N.; Reimann, W. *J. Organomet. Chem.* **1987**, *322*, 141−150.
(11) (a) 5-ring ether-chelated structures have been found for 1-lithio-1-(2-methoxyphenyl)-3,3-diphenylallene (Dem′yanov, P.; Boche, G.; Marsch, M.; Harms, K.; Fyodorova, G.; Petrosyan, V. *Liebigs Ann.* **1995**, 457−460), 3-lithio-1-methoxybutane[4d] and 2,2-bis(methoxymethyl)-1-lithiopropane.[4e] (b) 5- and 6-ring amine-chelated structures have been found for 1,1-bis(dimethylaminomethyl)-2-lithiopropane,[4f] *N*-(2-lithiocyclohexenyl)-*N*,*N*′,*N*′-trimethyl-1,3-propanediamine,[12a] and o-dialkylaminophenyllithium.[13a]
(12) (a) Polt, R. L.; Stork, G.; Carpenter, G. B.; Williard, P. G. *J. Am. Chem. Soc.* **1984**, *106*, 4276−4277. (b) Waldmüller, D.; Kotsatos, B.; Nichols, M. A.; Williard, P. G. *J. Am. Chem. Soc.* **1997**, *119*, 5479−5480. (c) Williard, P. G.; Liu, Q.-Y. *J. Am. Chem. Soc.* **1993**, *115*, 3380−3381.
(13) (a) Rietveld, M. H. P.; Wehman-Ooyevaar, I. C. M.; Kapteijn, G. M.; Grove, D. M.; Smeets, W. J. J.; Kooijman, H.; Spek, A. L.; van Koten, G. *Organometallics* **1994**, *13*, 3782−3787. (b) Jastrzebski, J. T. B. H.; van Koten, G.; Konijn, M.; Stam, C. H. *J. Am. Chem. Soc.* **1982**, *104*, 5490−5492. Wehman, E.; Jastrzebski, J. T. B. H.; Ernsting, J.-M.; Grove, D. M.; van Koten, G. *J. Organomet. Chem.* **1988**, *353*, 145−155.
(14) McDougal, P. G.; Rico, J. G. *J. Org. Chem.* **1987**, *52*, 4817−4819.

(15) See the Supporting Information for NMR spectra, simulations, and exchange matrixes.

Table 2. ^{13}C NMR Chemical Shifts of 2-Alkylphenyllithium Reagents.

RLi	solv.	*T*/°C	C-1	C-2	C-6	δ_{Li}[a]	J_{CLi} (^{6}Li)
			Monomers (p = PMDTA):				
$(PhLi)_1$[b]	THF	−111	196.4	143.2	143.2	1.15	15.3[c]
$(PhLi)_1$·p[b]	[d]	−125	196.5	143.8	143.8	1.95	15.6
$(\mathbf{7})_1$	[f]	−141	195.2	155.3	142.5	1.24	14.6[g]
$(\mathbf{2})_1$	[h]	−130	195.9	154.3	142.6	1.23	12[c]
$(\mathbf{2})_1$·p	[h]	−145	196.7	150.5	142.3	2.06	15.5[c]
$(\mathbf{3})_1$	[f]	−127	195.5	153.2	142.4	1.26	15[c]
$(\mathbf{3})_1$·p	[f]	−127	195.8	152.5	142.2	2.05	13.3[c]
$(\mathbf{4})_1$·p	[h]	−127	195.8	148.4	142.6	2.1	17[c]
$(\mathbf{5})_1$·p	[h]	−147	197.0	148.0	142.1	2.05	14.8[c]
$(\mathbf{6})_1$	[f]	−125	195.6	152.9	142.5	1.28	15
$(\mathbf{6})_1$·p	[f]	−125	195.7	152.2	142.3	2.1	[k]
			Dimers				
$(PhLi)_2$[b]	THF	−111	188.2	144.5	144.5	1.59	7.9[j]
$(\mathbf{7})_2$	[f]	−141	186.6	157.3	144.0	1.57	[k]
$(\mathbf{1})_2$ (**A**)[l]	[h]	−132	188.8	152.2	143.5	1.81, 3.84	7.0[j]
$(\mathbf{1})_2$ (**B**)[l]	[h]	−132	188.4	151.9	143.2	2.61	7.0[j]
$(\mathbf{1})_2$ (**C**)[l]	[h]	−132	[i]	151.2	143.0	2.90	[i]
$(\mathbf{2})_2$ (**A**)	[h]	−130	184.3	152.4	144.1	1.87, 1.96	7[j]
$(\mathbf{4})_2$ (B/C)	[f]	−127	186.1	149.7	143.1	2.38	8.1[j]
$(\mathbf{5})_2$ (B/C)	[f]	−127	188.2	152.4	143.2	1.74	8.1[j]
$(\mathbf{6})_2$ (X)[m]	Et_2O	−126	188.0	152.8	144.0	1.67	[k]
$(\mathbf{6})_2$ (Y)[m]	Et_2O	−126	186.8	153.7	144.2	1.50	[k]
Tetramers:							
$(PhLi)_4$[b]	Et_2O	−106	174.0	143.8	143.8	2.39	5.1

[a] Reference: 0.3 M LiCl in methanol. [b] Ref 1i. [c] 1:1:1 Triplet. [d] 2:1 THF/Me_2O. [e] 45:25:30 THF/Me_2O/Et_2O. [f] 3:2 THF/Et_2O. [g] Calculated from a measured J_{C-7Li} coupling of 38.5 Hz. [h] 3:2:1 THF/Me_2O/Et_2O. [i] Signal not found. [j] 1:2:3:2:1 quintet. [k] Splitting not resolved. [l] Ref 1h. [m] X is the minor and Y the major isomer (35:65).

between the steric effects of ortho substituents and their chelating effects, we have used several model systems. Phenyllithium (**8**) forms both monomers and dimers in THF (K_{MD} = 30 M^{-1} at −118 °C).[1i,16,17] In our mixed solvent system 3:2 THF/Et_2O K_{MD} = 208 M^{-1} at −128 °C. To mimic the steric effect of the chelating ortho substituents we have examined 2-ethylphenyllithium (**7**), which can be crystallized, unlike our previous model **9**.[1h] The reagent was mostly monomer in 3:2 THF/Et_2O, but a higher aggregate was easily detected, and shown to be a dimer by the concentration dependence of the ^{6}Li NMR signals (K_{MD} = 0.19 ± 0.04 M^{-1} at −140 °C, ca. 5% dimer at 0.14 M total lithium concentration). In this and previous papers[1c,h] we have made extensive use of two solvent mixtures which qualitatively show similar behavior: 3:2 THF/Et_2O, which can be used down to −140 °C, and 3:2:1 THF/Me_2O/Et_2O, which is fluid enough for high-resolution NMR work down to −155 °C. We find K_{MD} = 0.19 ± 0.03 M^{-1} at −139 °C for **7** in 3:2:1 THF/Me_2O/Et_2O. Thus, the two solvent mixtures are identical within experimental error in their ability to cause deaggregation, at least for this specific lithium reagent.

Interaction of 7 with PMDTA. The behavior of the chelated lithium reagents with PMDTA has in several cases provided an estimate of the strength of chelation, since the tridentate ligand is in competition with the chelating group. The PMDTA titration of **7** is very similar to other model systems (**8**, **9**) we have examined. The association constant is almost too large to measure. A solution of **7** at −127 °C with 1.06 equiv of PMDTA had 96% of ArLi complexed, giving K_{PMDTA} ([**7**·PMDTA]/[**7M**]·[PMDTA]) = 1880 M^{-1}.

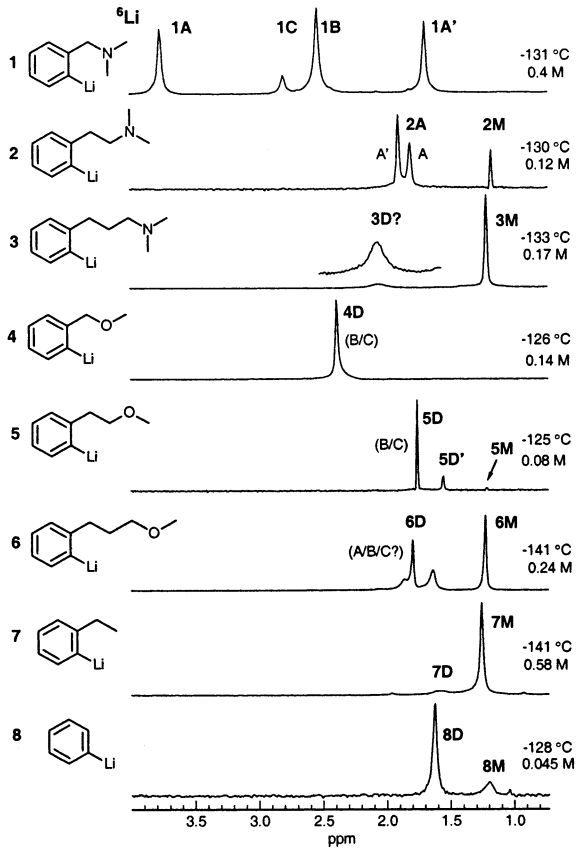

Figure 1. Low temperature ^{6}Li NMR spectra of lithium reagents **1**−**8** in 3:2 THF/Et_2O (**M** = monomer, **D** = dimer, for **A**/**B**/**C** see Scheme 2). Chemical shifts are referenced to external 0.3 M LiCl in methanol.

The dynamics of ligand exchange were readily measured by DNMR studies, either using ^{6}Li NMR spectra at 0.5 equiv of PMDTA, or the ^{13}C PMDTA signals with excess ligand present. Two ligand exchange processes were identified. At low temperature 9 signals were seen in the ^{13}C NMR spectra of the bound ligand, in addition to the 4 signals of free PMDTA (see Figure 2 for representative spectra).[15] Around −100 °C the bound ligand symmetrizes, with 9 signals going to 4. The central methyl signal is unaffected. We did not detect the two-phase process, first C−Li bond rotation then Me_2N−Li decoordination/inversion, that was seen for neopentyllithium·PMDTA.[7c] However, the free PMDTA NMe_2 signal interferes with detailed observation of the methyl coalescences in our study. At ca. −80 °C, bound and free PMDTA coalesce. This appears to be a simple dissociative process because the rates were identical for solutions containing 0.6 and 1.9 equiv of PMDTA,[15] where the concentration of free PMDTA differs by several orders of magnitude. Figure 3 shows an Eyring plot of the rate constants that were determined by a 6-spin DNMR simulation of the PMDTA CH_2 signals,[15] together with corresponding data for ligand dynamics in **4**·PMDTA and **5**·PMDTA.

Five-Membered Ring Amine Chelation−2-(Dimethylaminomethyl)phenyllithium (**1**). Previous work on **1** and its congeners[1h] has shown that these are mixtures of dimeric chelation isomers (**A**, **B**, and **C**, X = NMe_2, NEt_2, or NMe^iPr, Scheme 2),[18] with much lower rates of dimer to monomer

(16) (a) Bauer, W.; Seebach, D. *Helv. Chim. Acta* **1984**, *67*, 1972−1988. (b) Heinzer, J.; Oth, J. F. M.; Seebach, D. *Helv. Chim. Acta* **1985**, *68*, 1848−1862. (c) Seebach, D.; Hässig, R.; Gabriel, J. *Helv. Chim. Acta*, **1983**, *66*, 308−337.
(17) Bauer, W.; Winchester, W. R.; Schleyer, P. v. R. *Organometallics* **1987**, *6*, 2371−2379.

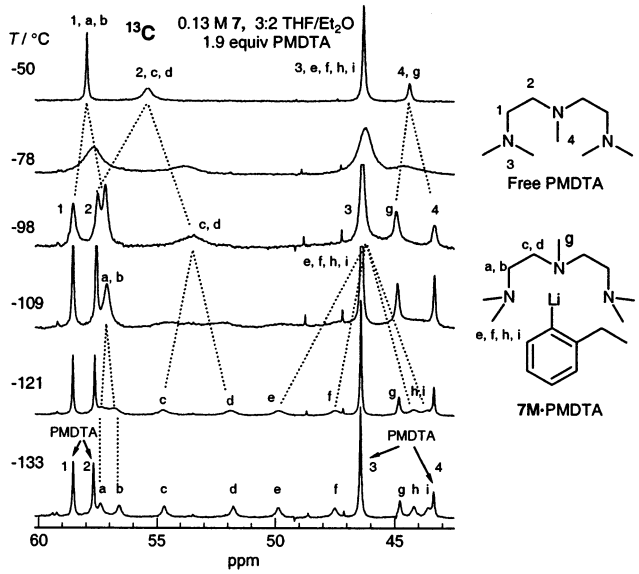

Figure 2. Variable temperature NMR study of [^{6}Li]**7** in 3:2 THF/Et_2O with 1.9 equiv of PMDTA. Line shape analysis[15] gave $\Delta H^{\ddagger} = 4.4 \pm 0.1$ kcal/mol, $\Delta S^{\ddagger} = -18 \pm 3$ eu for ligand symmetrization (k_{symm}) and $\Delta H^{\ddagger} = 7.1 \pm 0.1$ kcal/mol, $\Delta S^{\ddagger} = -10 \pm 1$ eu for ligand dissociation (k_{diss}).

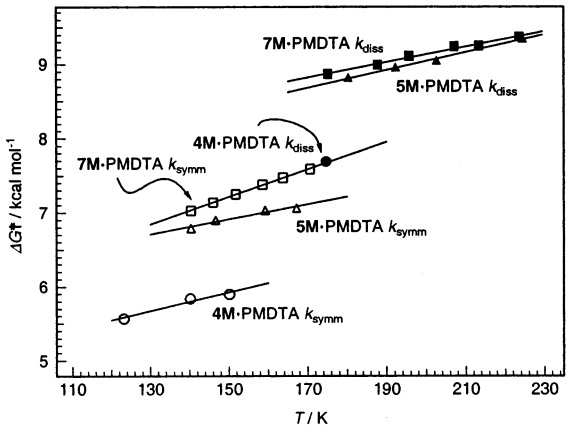

Figure 3. Eyring plot for rates of ligand symmetrization (k_{symm})and ligand dissociation (k_{diss}) of PMDTA complexes of **4**, **5**, and **7** ($\Delta G^{\ddagger}_{-100}$ for k_{symm} was 6.21, 7.14 and 7.64 and for k_{diss}, 7.69, 8.74 and 8.86 for **4**, **5**, and **7**, respectively).

Scheme 2. Dimeric Chelation Isomers.

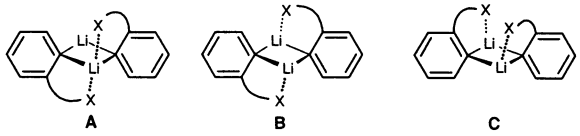

dissociation and much higher aggregation constants than the largely monomeric model systems. Of the several cosolvents tried (TMEDA, PMDTA, HMPA), only HMPA was capable of causing detectable deaggregation.

Six-Membered Ring Amine Chelation—2-(2-Dimethylaminoethyl)phenyllithium (2). Compound **2** showed two sets of signals in the ^{13}C and ^{6}Li NMR spectra (Figure 1).[15] The major component showed the characteristic C—Li quintet of a dimer at δ 184.3 in the ^{13}C NMR spectrum. Two closely spaced signals in the ^{6}Li NMR spectra maintained a 1:1 ratio independent of

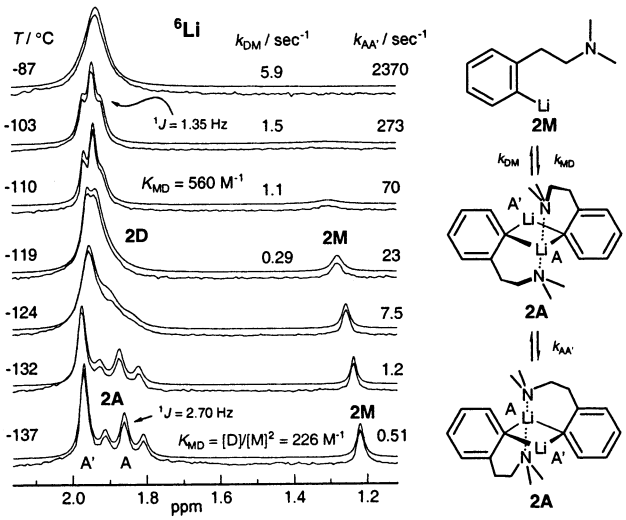

Figure 4. Selected ^{6}Li NMR spectra from a variable temperature experiment of 0.10 M [^{6}Li, ^{15}N]**2** in 3:2 THF/Et_2O. The upper trace of each pair is a simulated spectrum using the rate constants shown and the exchange matrix of Fig. S-2.[15]

concentration and were assigned to the two lithiums of a type A dimer (Scheme 2). The ^{6}Li signal at δ 1.87 is slightly broader than the one at δ 1.96, presumably due to residual ^{6}Li—^{14}N coupling. The minor component (^{6}Li δ 1.23) was assigned as a monomer. Because of the relatively low concentration of the monomer we were able to get only a poorly resolved 1:1:1 triplet signal for the C—Li carbon in the ^{13}C NMR spectra at δ 195.9, but all evidence is consistent with such an assignment. These assignments were confirmed by the variable temperature ^{6}Li NMR spectra of the ^{15}N—^{6}Li doubly labeled material (Figure 4).

Selected spectra from a variable temperature NMR study of the ^{15}N—^{6}Li doubly labeled compound are shown in Figure 4.[19] Below −128 °C the upfield ^{6}Li signal of the dimer is split into a 1:2:1 triplet ($J_{LiN} = 2.7$ Hz), thus confirming the **A** structure. It is unusual for N-coordination to result in an upfield ^{6}Li shift. Normally, both intramolecular[1b,1h] and intermolecular (with TMEDA and PMDTA[1i]) N-coordination results in downfield shifts. The monomer shows no hint of Li—N coupling in the ^{6}LiNMR spectra. The C—Li signal in the ^{13}C NMR spectra was not well resolved but showed signs of C—Li coupling, so intermolecular Li—Li exchange is not the reason that Li—N coupling is absent. *We conclude that the monomer, unlike the dimer, is not chelated.*

Scheme 3 presents a scenario for the effect of chelation on the monomer—dimer equilibrium, and our best estimates for the fractions of the two species in brackets that are not observable.[15] We estimate K_{chel} ([chelated]/[unchelated]) as ≥ 25 for the dimer and ≤ 0.18 for the monomer. The hypothetical monomer—dimer equilibrium constant K_{MD} ([D]/[M]^2) with both monomer and dimer chelated is estimated at ≥ 10 000 M^{-1}, and with both monomer and dimer unchelated, ≤ 0.24 M^{-1}. The latter value is quite consistent with the measured K_{MD} of 0.19 M^{-1} for the model system 2-ethylphenyllithium. These numbers illustrate the dramatic influence of chelation on the monomer—dimer equilibrium, a switch of a factor of at least 40 000 in K_{MD} and almost 3 kcal/mol in $\Delta\Delta G°$.

(18) (a) Chelation isomers of a similar type have been identified for tetrameric 3-dimethylaminopropyllithium,[4g] and dimeric 1,1-bis(dimethylaminomethyl)-2-lithiopropane[4f] and 3-lithio-1,5-dimethoxypentane.[4h]

(19) Other examples of ^{6}Li—^{15}N coupling in amine chelates have been reported.[8,12b,20,21,22a]

Scheme 3. Estimated Dimerization and Chelation Equilibrium Relations for 0.10 M (total ArLi) **2** in 3:2 THF/Et_2O at −137 °C[a]

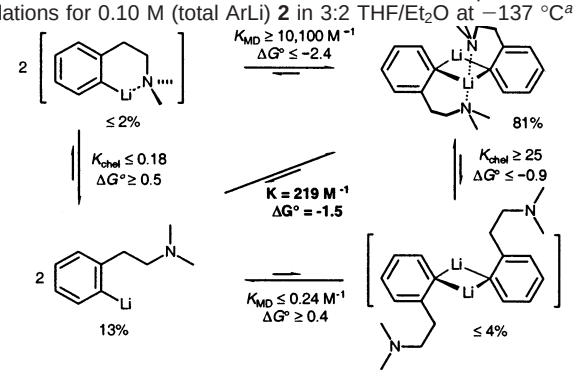

[a] The items in square brackets were not detected, and the K_{eq}s involving these species are based on estimates of their maximum likely concentration.[15]

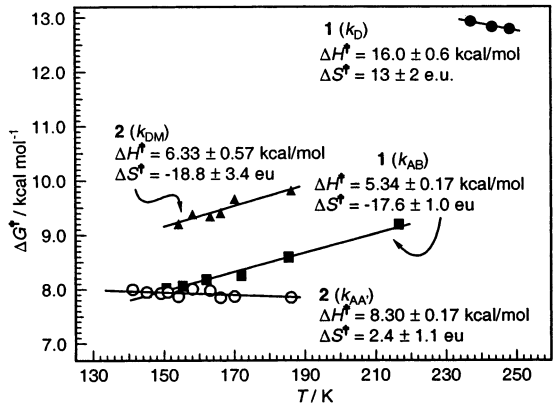

Figure 5. Rates of intra- and intermolecular exchanges of **2** in 3:2 THF/Et_2O compared with a related processes in **1**.[1h] $k_{AA'}$: intramolecular exchange between two Li signals of **2A**; k_{AB}: intramolecular exchange of the A and B chelation isomers of the dimer of **1**; k_{DM}: dimer to monomer exchange of **2**; k_D: loss of coupling of C−Li carbon in the dimer of **1** (associative through trimer or tetramer).[1h]

Dynamic Processes for 2. Two dynamic processes are seen for **2** (Figure 4). First, the singlet and triplet in the ^{15}N labeled **A**-dimer coalesce to form a new triplet (in the unlabeled compound the two singlets coalesce to one). This is the result of intramolecular exchange of the chelating ligands between the two sites, so that each lithium becomes coupled equally to both nitrogens, now with half the coupling constant. The second process is the coalescence of the dimer signals with that of the monomer, the result of intermolecular exchange. We have simulated the spectra by treating the **A**-dimer singlet as a 1:2:1 triplet with $J_{LiN} = 0$,[1k] and allowing pairwise exchange of the equivalent signals in the two "triplets."[15] This simulation provided an excellent fit between calculated and experimental spectra confirming the assignment of the complex changes in line shapes. The free energies of activation for the degenerate chelation isomerization of **2** are similar to those found for the intramolecular interconversion of the chelation isomers of **1**, although this compound shows a substantial negative $\Delta S^‡$, whereas **2** has $\Delta S^‡$ of essentially 0 (Figure 5). This suggests that for **1** the dechelation requires association of one or more additional solvent molecules at the transition state, whereas for **2** this is a unimolecular process.

As is often the case,[1d,7c,16b,c,23−25] the higher aggregate of **2** was favored at higher temperature (aggregation releases solvent molecules), from about 14% monomer at −137 °C in the sample of Figure 4 ($K_{MD} = [D]/[M]^2 = 226\ M^{-1}$) to about 9% at −110 °C ($K_{MD} = 560\ M^{-1}$). Simulation of the spectra also gave values for the rates of dimer-monomer equilibration. Figure 5 shows a $\Delta G^‡$ vs T plot of the data obtained. The negative entropy of activation implies that solvent assists in the dimer to monomer process, as expected for a dissociative process. Note that **1** has an opposite temperature dependence of $\Delta G^‡$ (positive $\Delta S^‡$), consistent with the known associative nature of that process.[1h]

Interaction of 2 with TMEDA. The incremental addition of TMEDA to a sample of **2** produced changes in the NMR spectra consistent with complexation with both the monomer and dimer. A new set of triplet and singlet signals appeared in the ^6Li NMR spectra downfield of the original ones, assigned to **2A**·TMEDA (**2A**·*t* in Figure 6). The monomer signal broadens and moves steadily downfield. Apparently the complexed and uncomplexed monomers are in rapid equilibrium at −134 °C (as they are for PhLi·TMEDA[1i] and 2-isopentylphenyllithium·TMEDA[1h]). Figure 6 also shows spectra of a similar sample with 2 equiv of TMEDA at lower temperatures. The signals decoalesced at −140 °C and are well resolved at −153 °C. The TMEDA-complexed monomer (**2M**·TMEDA) is not chelated. The complexation is sub-stoichiometric. With two equiv of TMEDA 52% of the lithium species are coordinated to TMEDA.

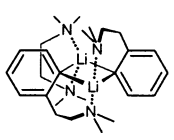

2A-TMEDA

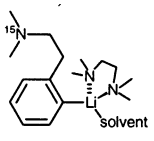

2M·TMEDA

We have determined by line-shape simulation the relative proportions of the four species (M, M_t, D, D_t) in the spectrum at −153 °C at 2 equiv of TMEDA, and have estimated monomer−dimer association constants for the TMEDA complexed species ($K_{MD} = [D_t]/[M_t]\ [M] = 64\ M^{-1}$) and the THF complexed species ($K_{MD} = 170\ M^{-1}$). Similarly, we can define the TMEDA affinity of the monomer ($K = [M_t]/[M]\ [t] = 11\ M^{-1}$) and for the dimer ($K = [D_t]/[D]\ [t] = 4\ M^{-1}$). Thus, TMEDA shows approximately a 3-fold higher affinity for the monomer than for the dimer.

Interaction of 2 with PMDTA. Figure 7a shows the effect of the addition of PMDTA to a sample of [^6Li,^{15}N]**2**. The new sharp singlet at δ 2.1 was assigned to the PMDTA complex. There is no detectable Li−N coupling, so the complexation forms monomeric unchelated **2**·PMDTA.

The PMDTA titration experiment also provided an opportunity to determine the molecularity of the two species we

(20) Huls, D.; Günther, H.; van Koten, G.; Wijkens, P.; Jastrzebski, J. T. B. H. *Angew. Chem., Int. Ed. Engl.* **1997**, *36*, 2629−2631.

(21) Eriksson, J.; Arvidsson, P. I.; Davidsson, Ö. *J. Am. Chem. Soc.* **2000**, *122*, 9310−9311.

(22) (a) Aubrecht, K. B.; Lucht, B. L.; Collum, D. B. *Organometallics* **1999**, *18*, 2981−2987. (b) Romesberg, F. E.; Gilchrist, J. H.; Harrison, A. T.; Fuller, D. J.; Collum, D. B. *J. Am. Chem. Soc.* **1991**, *113*, 5751−5757. (c) Remenar, J. F.; Lucht, B. L.; Kruglyak, D.; Romesberg, F. E.; Gilchrist, J. H.; Collum, D. B. *J. Org. Chem.* **1997**, *62*, 5748−5754. (d) In other systems, TMEDA competes less well: Collum, D. B. *Acc. Chem. Res.* **1992**, *25*, 448−454. (e) Lucht, B. L.; Bernstein, M. P.; Remenar, J. F.; Collum, D. B. *J. Am. Chem. Soc.* **1996**, *118*, 10 707−10 718. (f) Kim, Y− J.; Bernstein, M. P.; Roth, A. S. G.; Romesberg, F. E.; Williard, P. G.; Fuller, D. J.; Harrison, A. T.; Collum D. B. *J. Org. Chem*. **1991**, *56*, 4435−4439.

(23) Knorr, R.; Freudenreich, J.; Polborn, K.; Nöth, H.; Linti, G. *Tetrahedron* **1994**, *50*, 5845−5860.

(24) Vinyllithium also complexes with PMDTA as a dimer. It was not established whether the complexation of the PMDTA was bidentate or tridentate. Bauer, W.; Griesinger, C. *J. Am. Chem. Soc.* **1993**, *115*, 10 871−10 882.

(25) Harder, S.; Boersma, J.; Brandsma, L.; Kanters, J. A.; Bauer, W.; Schleyer, P.v. R. *Organometallics* **1989**, *8*, 1696−1700.

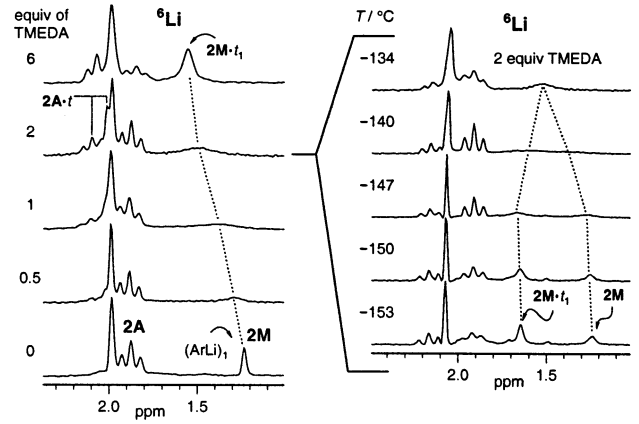

Figure 6. ^{6}Li NMR spectra. Left panel: TMEDA titration of a 0.16 M solution of [^{6}Li, ^{15}N]**2** in 3:2 THF/Et_2O at −134 to −137 °C. Right panel: a variable temperature study of a similar sample (0.13 M in 3:2:1 THF/Me_2O/Et_2O) with 2 equiv of TMEDA, showing decoalescence of the TMEDA complexed and uncomplexed monomers (t = TMEDA, M = monomer).

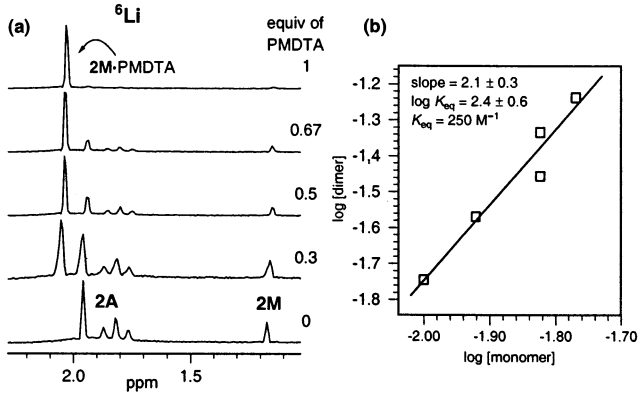

Figure 7. (a) ^{6}Li NMR spectra of a PMDTA titration of a 0.13 M solution of doubly labeled [^{6}Li,^{15}N]**2** in 3:2:1 THF/Me_2O/Et_2O at −145 °C. (b) Concentration dependence of the uncomplexed monomer and dimer signals during the PMDTA titration.

have assigned as the monomer and dimer of **2**. A log−log plot of the concentrations of the non-PMDTA complexed species (signals at δ 1.2 vs δ 1.7−2.0) gave a slope of 2.1, confirming the assignment of aggregation states (Figure 7b).

Seven-Membered Ring Amine Chelation—2-(3-Dimethylaminopropyl)phenyllithium (**3**). ^{13}C and ^{6}Li NMR studies of **3** show chemical shifts and couplings characteristic of a monomer (C−Li δ 195.5, 1:1:1 triplet, J_{C-Li} = 15 Hz). There is no detectable ^{6}Li−^{15}N coupling in either THF/Et_2O media or solutions with TMEDA, PMDTA, or HMPA added, so the compound exists largely in an unchelated form. A small broad signal attributable to a dimer appears at δ 2.1 in the ^{6}Li NMR spectra amounting to 6−8% of the area of the monomer, which would give a monomer−dimer association constant K_{MD} = 0.27 M^{-1}. Concentration-dependent studies were not done to support such an assignment. If this signal corresponds to a dimer, the substantial downfield shift compared to model compounds, where the dimer signal appears at δ 1.5−1.6 (see Figure 1), suggests that it is chelated.

PMDTA complexed stoichiometrically to **3** (Figure 8a). HMPA also formed a stoichiometric mono-complex. Past one equiv a substantial amount of triple ion Ar_2Li^- $Li(HMPA)_4^+$ was formed, with a singlet at δ 3.8 and quintet at δ −0.4 in ^{6}Li NMR spectra.

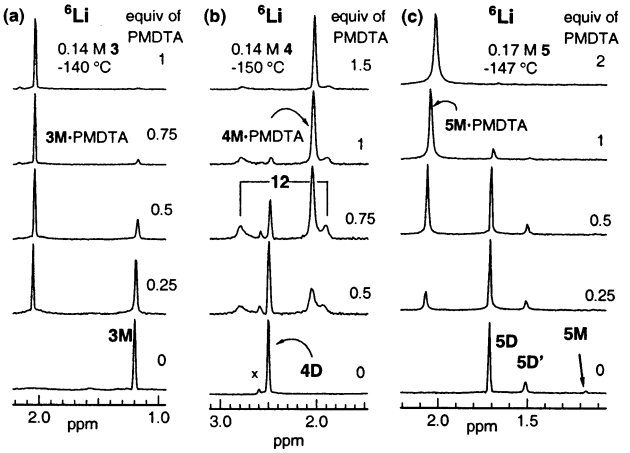

Figure 8. ^{6}Li NMR spectra showing the effect of PMDTA on solution in 3:2:1 THF/Me_2O/Et_2O of (a) [^{6}Li, ^{15}N]**3** (the indicated equiv of PMDTA are low by ca. 20%); (b) [^{6}Li]**4** (c) [^{6}Li]**5**.

Five-Membered Ring Ether Chelation—2-(Methoxymethyl)phenyllithium (**4**). Only a single species is detectable in solution of **4** in THF mixed solvents. The compound is aggregated as judged by the ^{13}C NMR signal of the C−Li carbon at δ 186.1, a 1:2:3:2:1 quintet (J_{C-6Li} = 7.6 Hz). Both the chemical shift and the coupling pattern are consistent with a cyclic dimer, but higher cyclic oligomers have not been ruled out. No signal that could be identified as a monomer was found in the ^{13}C and ^{6}Li NMR studies carried out on **4**. The tallest peak/noise signal between δ 0.5 and δ 2.0 in the spectrum of **4** in Figure 1 has 0.5% of the peak height of the major dimer signal. If we conservatively estimate that no more than 1% of monomer could be present, we calculate $K_{MD} \geq 35\,400$ M^{-1}.

It is much harder to get direct evidence for or against chelation in the ethers than for the amine chelates, since there is no suitable oxygen isotope for high-resolution NMR studies which would detect J coupling between Li and oxygen. The single ^{6}Li chemical shift of δ 2.4 is not directly useful for structure assignment, since it is possible that conformational isomers of the **A**/**B**/**C** type are in rapid equilibrium. Such equilibration is supported by the proton NMR signal of the benzylic CH_2 group, which appeared as a singlet at δ 4.70 even at −151 °C.[15]

Dynamic Processes for 4. We have estimated the barrier to aggregate equilibration of **4** from collapse of the C−Li coupling (1:2:3:2:1 quintet to singlet). Sample spectra, simulations and exchange rate constant data in the form of a $\Delta G^{\ddagger}$ vs T plot are shown in Figure 9. The OMe chelated compound **4** is substantially more labile than **1** (barriers ca. 3 kcal/mol lower), and shows the opposite sign for $\Delta S^{\ddagger}$. This may indicate a different mechanism for the interaggregate exchange of **1** and **4**. The exchange of **1** is faster at higher concentrations, consistent with an associative process going through higher aggregates. We have not measured the concentration dependence for **4**, but the large negative entropy is consistent with coordination of additional solvent in the transition state for dimer dissociation. However, we do not want to over-interpret the $\Delta S^{\ddagger}$ values. The changes in line shape are relatively small, and obtaining accurate rates is hampered by the long acquisition times required, typically 30−100 min, resulting in some temperature drift during the experiment. The internal ^{13}C chemical shift thermometer tris(trimethylsilyl)methane[1j] effectively corrects for small temper-

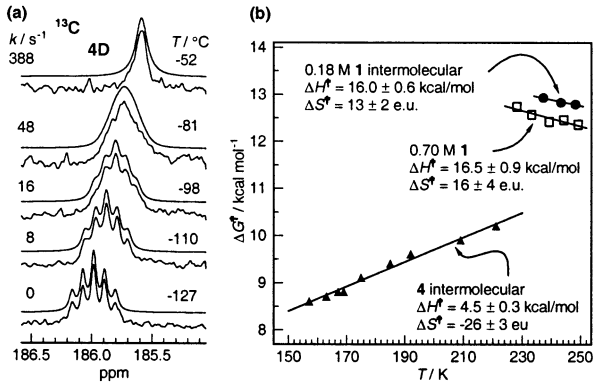

Figure 9. (a) Selected variable temperature ^{13}C NMR spectra of the C−Li carbon of 0.15 M [^{6}Li]**4** in 3:2:1 Me_2O/THF/Et_2O. The simulated spectra (upper trace of each pair) were obtained using the 6 × 6 exchange matrix reported previously.[1h] (b) Eyring plots and activation parameters for the intermolecular exchange rate ($\Delta G^{\ddagger}_{-65}$ = 9.9 kcal/mol). Related processes for **1** in 3:2 THF/Et_2O are also shown in the graph for comparison.

ature drifts to provide time-averaged temperatures, but it was not available for this experiment.

Interaction of 4 with TMEDA. In contrast to the amine analogue **1**, which complexes modestly with TMEDA, spectra of **4** gave no indication of interaction with TMEDA.[15] The failure to form a TMEDA complex is unlikely to have steric origins since other ortho-substituted lithium reagents such as **1** or **2** complex reasonably well and are at least as crowded. We conclude that **4** must be chelated and have a strong preference for the **B** and/or **C** isomers (Scheme 2), which cannot form bidentate complexes with TMEDA, over the **A** structure.

Interaction of 4 with PMDTA. Given the absence of significant interaction with TMEDA, it is surprising that **4** complexed strongly with PMDTA. The spectroscopic details of the interaction were apparent only at very low temperatures (−150 °C). Two species are formed, one gives a 1:1 ratio of two peaks in the ^{6}Li NMR spectra (Figures 8b and 10), and the second gives a singlet δ 2.04. The ratio of the two sets of peaks changes to favor the singlet at higher concentration of PMDTA, in a way consistent with formulating it as a monomer, and the other species as a dimer. Both species have unexpected spectroscopic features.

The first species to be formed gives a 1:1 ratio of two peaks at δ 1.9 and 2.8 at −150 °C. An unusual bonding situation is indicated by the very low temperatures (< −140 °C) required to decoalesce the various solvated species. In contrast, the PMDTA complexes of **1**,[1h] **2**, **3**, **5**, **6**, **7**, PhLi[1i] and other lithium reagents,[7b,c] are much less labile. We have considered three precedented structures for **4D**·PMDTA: a triple ion **10**,[1d] an **A**-type dimer **11**, and an open dimer structure **12** (Figure 10c).

The triple ion structure **10** can be ruled out. The ^{6}Li chemical shift of SIP−PMDTA complexes (e.g., Li·PMDTA^{+} // $^{-}$C(SiMe$_3$)$_3$) is close to δ 0, whereas the species here has shifts of δ 2−3. Furthermore, all of the ^{13}C NMR signals in the less polar solvent 2:1 Me_2O/Et_2O, where a higher fraction of the **4D**·PMDTA complex formed and the rates are slower, are doubled. The ipso carbon signals are especially revealing: at δ 193.2 (distorted 1:1:1 triplet) and δ 188.0 (coupling unresolved), quite close to the PMDTA-monomer signal at δ 195.8 and the non-PMDTA-dimer signal at δ 185.3 (Figure 10a). The substantial chemical shift difference of 5.1 ppm between the ipso carbons argues against assignment of an **A**-type dimer **11** in

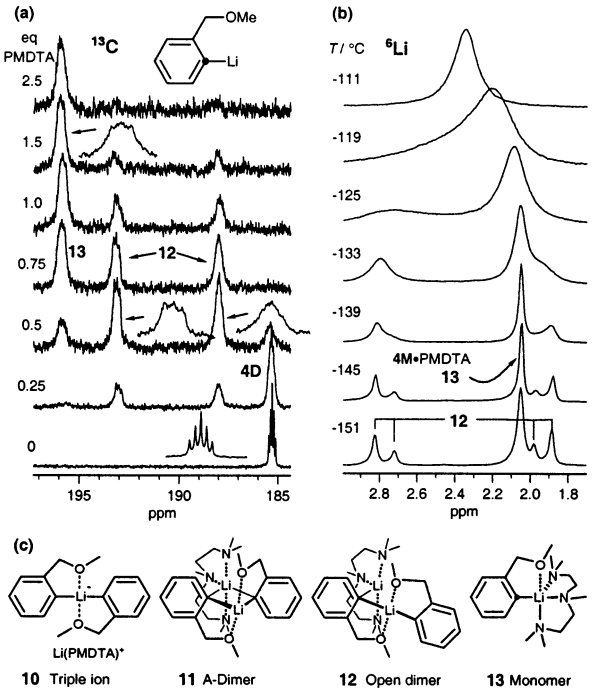

Figure 10. NMR studies of a 0.33 M solution of [^{6}Li]**4** in 2:1 Et_2O/Me_2O. (a) ^{13}C spectra of a PMDTA titration at −135 °C. (b) Variable temperature ^{6}Li NMR study of the sample containing 0.75 equiv of PMDTA. (c) Possible structures for the **4**-PMDTA species.

which a restricted conformation of the PMDTA ligand makes the two rings diastereotopic. We conclude that the **4D**·PMDTA complex has an open dimer structure **12** where one of the C−Li signals mimics that of the monomer, whereas the other resembles the dimer. Open dimers have been detected for lithium diisopropylamide and other lithium amides,[22b,c,12c] but not for organolithium reagents.[24]

Both the ^{6}Li and the ^{13}C spectra of the PMDTA-dimer showed distortions in peak shape at −140 °C. The origin of these distortions became apparent when the samples were cooled further. Each of the ^{6}Li peaks decoalesced to an approximately 2:1 ratio of singlets (Figure 10b). We have not established the origin of this dynamic process, with $\Delta G^{\ddagger}_{-141}$ = 7.1 kcal/mol. Slowing of some conformational change within either the PMDTA ligand or the MeO groups, or restricted rotation around the C−Li(PMDTA) bond[7c] are possible explanations.

The second species which forms on treatment of **4** with PMDTA gives a singlet at δ 2.04 in the ^{6}Li NMR spectrum and is formed to the extent of 70% at one equiv and 91% at 3 equiv in 3:2:1 THF/Me_2O/Et_2O solvent. The C−Li carbon chemical shift (δ 195.8) and coupling (1:1:1 triplet, J_{C-Li} = 17 Hz for ^{6}Li) are consistent with a monomeric PMDTA complex. The PMDTA must be coordinating lithium in a tridentate fashion, otherwise TMEDA would have given a similar effect.

We also conclude that the lithium in **4M**·PMDTA is still chelated to the CH_2OMe group (structure **13**), based on the peculiar properties of the PMDTA ligand signals in the ^{13}C NMR spectra. In complexes of **2**, **3**, **5**, **6** and **7** with PMDTA the complexed ligand shows 9 resolved signals at temperatures between −130 and −145 °C (Figures 2 and 11).[26] In contrast, it is necessary to cool a sample of **13** to −150 °C to decoalesce

(26) Similar spectra have been reported for mesityllithium·PMDTA[7b] and neopentyllithium·PMDTA.[7c]

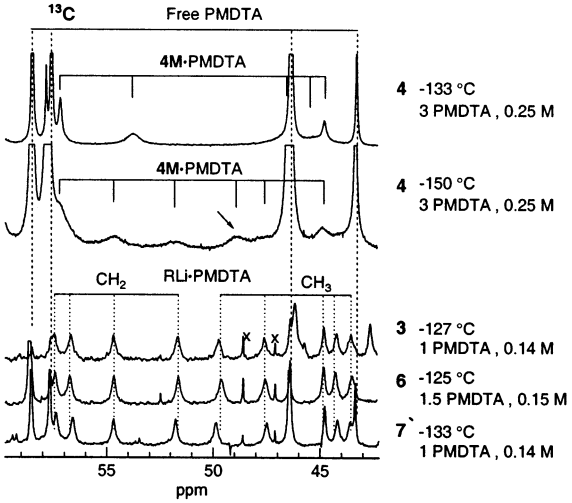

Figure 11. Ligand ^{13}C signals of the monomeric PMDTA complexes of **3**, **4**, **6**, and **7**. The spectra of **4** were measured in 3:2:1 THF/Me_2O/Et_2O, the others in 3:2 THF/Et_2O.

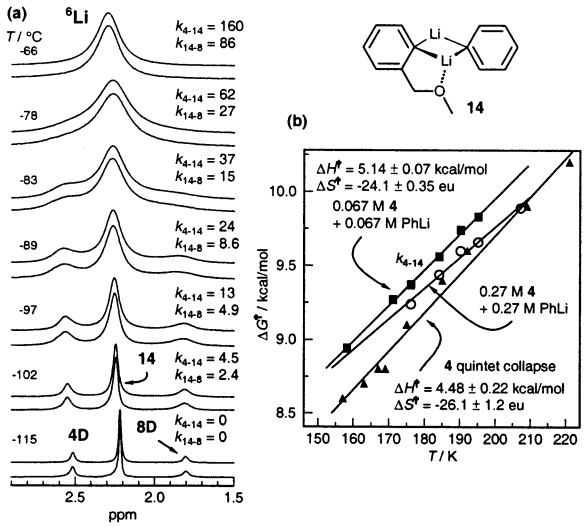

Figure 12. (a) Variable temperature NMR study of a solution containing 0.27 M [^{6}Li]**4** and 0.27 M [^{6}Li]PhLi in 3:2 THF/Et_2O. The upper trace of each set was a 3-spin DNMR simulation[1k] performed using the rate constants shown. The *k* values are the NMR rate constants for interchange of nuclei; the physical rate constants for interchange of dimer molecules would be half these values. (b) Eyring plots for the intermolecular exchanges of **4**.

the signals, and then only six of nine peaks, still broadened by exchange, are resolved for the bound PMDTA carbons. Like **7**·PMDTA (Figure 2), **4**·PMDTA shows two dynamic processes in the PMDTA ligand, symmetrization and intermolecular exchange (dissociation), except that the barriers are at least 1 kcal/mol lower than for **7**·PMDTA and other models (Figure 3). In addition, at least one of the signals (arrow in Figure 11) is shifted by ca. 1 ppm from that of the other complexes, which all have nearly identical ligand shifts. The methoxy group must be chelated in **13**, giving a rare structure with pentacoordinate lithium. Previously reported RLi·PMDTA complexes have been tetracoordinate at Li.[7c,27]

Mixed Dimer of 4 with Phenyllithium. The paucity of information that deals directly with the issue of chelation in **4** encouraged us to examine the mixed dimer of **4** and PhLi. Like **1**,[1h] solutions of **4** containing PhLi (**8**) show signals in the ^{6}Li and ^{13}C NMR spectra consistent with the formation of a mixed dimer **14** (Figure 12a) in higher than statistical amounts. The comproportionation equilibrium constant ([**14**]^2/[**4D**][**8D**]) is 17; statistical is 4. The mixed dimer would be expected to show two signals in the lithium NMR spectra (as does the mixed dimer of **1**). Since only one new signal for **14** is seen, ligand reorganization must be fast on the NMR time scale at −137 °C. An accidental equivalence is unlikely since the chemical shifts of the homodimers are separated by 0.7 ppm.

At higher temperatures the signals of **4D**, **14** and **8D** coalesce. A 3-spin DNMR simulation gave an excellent fit using only two rate constants, conversion of **4D** to **14** (k_{4-14}), and conversion of **14** to **8D** (k_{14-8}). A study of the concentration dependence gave ambiguous results (a 4-fold dilution led to a reduction in exchange rates by a factor of 1.2 to 1.6, suggesting at least some involvement of associative processes (e.g., mixed trimers) in the exchange. Unfortunately, there is not a direct connection between these rate constants and the physically real rate constants of aggregate exchange, because these must involve species (most likely monomers, but mixed trimers and tetramers are also plausible) which are not detectable and so cannot be incorporated into the simulation. However, the values obtained for k_{4-14} should approximate the values for aggregate exchange of **4D**. In fact, they are within a factor of 2 of those measured from collapse of the C−Li multiplet in a slightly different solvent mixture (3:2:1 Me_2O/THF/Et_2O vs 3:2 THF/Et_2O for the mixed dimer experiment, Figure 12b). Thus, this experiment provides a way of estimating the kinetic stability of dimers for which other techniques are not available. A similar mixed dimer experiment for **5** described below was more informative since here the monomeric species can be detected and explicitly incorporated into the simulations.

Six-Membered Ring Ether Chelation—2-(2-Methoxyethyl)phenyllithium (5). The homologue of **4**, compound **5**, shows none of the anomalous behavior exhibited by **4**. Two sets of signals in a 4:1 ratio were observed in the ^{6}Li and ^{13}C NMR spectra (Figure 13), and this ratio was concentration independent. We were unable to resolve the C−Li coupling, but the line shape and ^{13}C chemical shift (δ 188.2) of the C−Li carbon are very similar to those observed for other dimers (Table 2). We conclude that **5** is a mixture of two dimers, probably of the **B**/**C** type. A small signal at δ 1.2 was assigned to the monomer, but this could not be confirmed by observing the key ^{13}C signal for the C−Li carbon. Its intensity varied as expected for a monomer.[15] Our best value for K_{MD} is 11 000 M^{-1} at −121 °C in 3:2 THF/Et_2O, almost 5 orders of magnitude higher than the model systems (K_{MD} < 0.2 M^{-1}), and almost 2 orders of magnitude higher than the amine analogue **2** (K_{MD} = 240 M^{-1}).

Dynamic Processes for 5. Excerpts from a variable temperature experiment are shown in Figure 13. The signals for the two dimers **5D** and **5D′** coalesced at ca −110 °C, the monomer **5M** coalesced with the dimers above −90 °C. We did not perform the DNMR experiment at other concentrations to determine the molecularity of the exchange processes.

Interaction of 5 with TMEDA. Treatment of solutions of **5** with up to 8 equiv of TMEDA gave no significant change in

(27) Rüffer, T.; Bruhn, C.; Maulitz, A. H.; Ströhl, D.; Steinborn, D. *Organometallics* **2000**, *19*, 2829−2831. Schümann, U.; Kopf, J.; Weiss, E.; *Angew. Chem.* **1985**, *97*, 222; *Angew. Chem., Int. Ed. Engl.* **1985**, *24*, 215−216. Lappert, M. F.; Engelhardt, L. M.; Raston, C. L.; White, A. H. *J. Chem. Soc., Chem. Commun.* **1982**, 1323−1324. Karsch, H. H.; Zellner, K.; Mikulcik, P.; Lachmann, J.; Müller, G. *Organometallics* **1990**, *9*, 190−194.

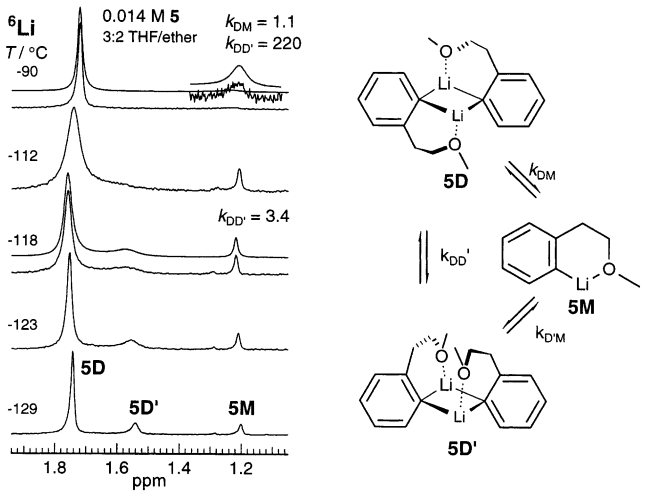

Figure 13. Variable temperature ^{6}Li NMR study of [^{6}Li]**5**. The upper trace for the −118 and −90 °C spectra are 3-spin DNMR simulations which give $\Delta G^{\ddagger}_{-118}$ (D−D′) = 8.50 kcal/mol and $\Delta G^{\ddagger}_{-90}$ (D−M) = 10.51 kcal/mol.

Scheme 4. Thermodynamic Relations in the PMDTA Complexes of **5** and **7**[a]

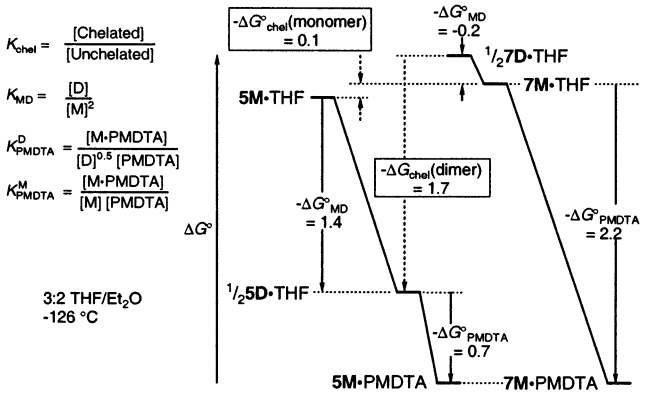

[a] The dotted arrows are not true equilibria, they indicate predicted free energy relations between **7** and the unchelated model for **7** (**5**).

the spectra.[15] Because TMEDA complexes well to similarly hindered ArLi reagents such as **2** and **9**,[1h] the failure to form significant amounts of a type **A**·TMEDA complex suggests strongly that the dimers must be of the **B**/**C** type (Scheme 2), as also observed for **4**.

Interaction of 5 with PMDTA. Figure 8c shows a ^{6}Li NMR study of a PMDTA titration of **5**. A monomeric complex is formed which has nearly identical ligand chemical shifts to the model systems **3** and **7** (see Figure 11), and thus is not chelated. However, complexation is no longer stoichiometric. In a solution of **5** containing 2.1 equiv of PMDTA at −126 °C 88% of ArLi was complexed, giving a K_{PMDTA} (Scheme 4) of 9.5 M^{-1}, whereas solutions of **7** had K_{PMDTA} = 1880 M^{-1}. These data, combined with the measured K_{MD} values for **5** (11 000) and **7** (0.19) can be used to construct the free energy diagrams shown in Scheme 4. If we assume that **5M** and **5D**, were they not chelated, would behave identically to the model **7** aggregates, we can conclude that **5D** is stabilized to the extent of 1.7 kcal/mol by chelation, whereas **5M** is negligibly stabilized (0.1 kcal/mol in the diagram, but the errors are at least ± 0.1 kcal/mol).

The dynamics of the PMDTA ligand are affected in only a minor way by chelation (Figure 3). In contrast to **4**·PMDTA, the intermolecular exchange of PMDTA (k_{diss} in Figure 3, $\Delta H^{\ddagger}$ = 5.4 ± 0.3 kcal/mol, $\Delta S^{\ddagger}$ = −10 ± 2 eu) was essentially identical to that of the model system, whereas the symmetrization of the ligand (k_{symm}, $\Delta H^{\ddagger}$ = 6.7 ± 0.2 kcal/mol, $\Delta S^{\ddagger}$ = −12 ± 1 eu) was faster by a factor of 2−4.

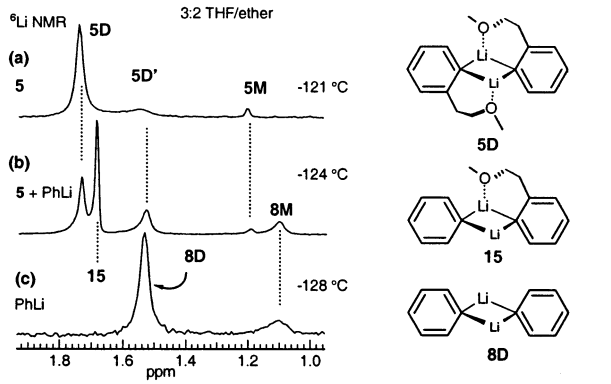

Figure 14. ^{6}Li NMR spectra in 3:2 THF/Et_2O. (a) 0.026 M **5** at −121 °C. (b) 0.01 M PhLi (**8**) and 0.01 M **5** at −124 °C. (c) 0.045 M PhLi at −128 °C.

Mixed Dimer of 5 with Phenyllithium. Some additional insights into the effects of chelation were obtained from a study of the mixed dimer of PhLi with **5**. A spectrum from such an experiment, together with spectra of the constituents, is shown in Figure 14. Signals for both monomer and dimer of **5**, the mixed dimer **15**, and monomer and dimer of PhLi can be seen. Line shape simulation of the signals in Figure 14b allowed calculation of the following monomer−dimer K_{MD} values ([D]/[M]^2): for **5**: 14 000 M^{-1}; for **15**: 3800 M^{-1}; for **8** (PhLi): 240 M^{-1}. Thus the monomer−dimer association constant goes up by about an order of magnitude for each chelating methoxyethyl group.

Dynamic NMR studies of solutions of **5**/PhLi (Figure 15) were complicated by the small area of the monomer signals, the superposition of the signals for **8D** (PhLi) and **5D′**, the chronic difficulty in assigning inherent line widths to the ^{6}Li signals, and the large number of adjustable parameters inherent in a 6-spin simulation (15 rate constants, 6 line widths, 6 chemical shifts and 6 populations). We made the following simplifying assumptions. Because of the low-temperature coalescences of **8D** and **8M**, and the two dimers **5D** and **5D′**, their relative chemical shifts, line widths, and populations are poorly defined through most of the temperature range. These were set from the low-temperature spectra and changed minimally during the simulation. Only four rate processes of the 15 possible were allowed: the interconversion of **5D** and **5D′**, the dissociation of **5D** to **5M** (both isomers of the dimer at the same rate), the dissociation of **8D** to **8M** and the dissociation of mixed dimer **15** to the two monomers (i.e., no bimolecular exchanges between the three dimers). It was possible to achieve satisfactory simulations throughout the temperature range (Figure 15) despite the drastically reduced set of adjustable parameters.

The variable temperature spectra showed a series of four coalescences: first the monomer and dimer of PhLi, and in the same temperature regime (−100 °C), the two dimers of **5** coalesced with each other. Then, between −93 and −74 °C the mixed dimer **15** coalesced with the averaged PhLi signals (and presumably also with **5M**, but this cannot be directly observed). Finally, between −52 and −41 °C, the averaged signals of **5** coalesced with the rest. The rates measured in this experiment

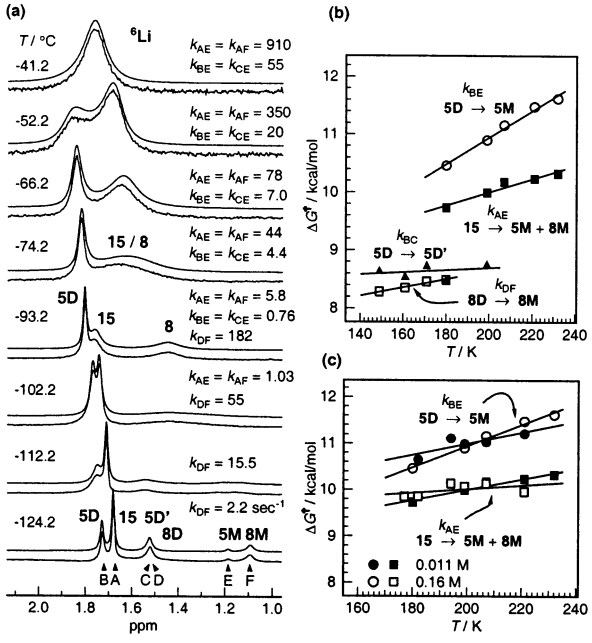

Figure 15. (a) Variable temperature ^{6}Li NMR study of a solution 0.011 M in **5** and 0.011 M in PhLi (**8**) in 3:2 THF/Et_2O. The upper trace at each temperature is the 6-spin DNMR simulation. The rate constants shown are the NMR rates. The physical rate constants for dissociation of **5D** and **8D** (k_{BE} and k_{DF}) are 0.5 times the values shown. (b) Eyring plot of the four independent rate constants used in the simulation: dissociation of **5D** ($k_{BE} = k_{CE}$, $\Delta H^‡ = 6.34 \pm 0.31$ kcal/mol, $\Delta S^‡ = -23.0 \pm 1.5$ eu); dissociation of **8D** (k_{DF}, $\Delta H^‡ = 7.21 \pm 0.15$ kcal/mol, $\Delta S^‡ = -7.2 \pm 0.9$ eu); dissociation of the mixed dimer **15** ($k_{AE} = k_{AF}$, $\Delta H^‡ = 7.74 \pm 0.33$ kcal/mol, $\Delta S^‡ = -11.3 \pm 1.6$ eu); interconversion of the two isomeric dimers of **5** (k_{CD}, $\Delta H^‡ = 8.31 \pm 0.56$ kcal/mol, $\Delta S^‡ = -1.9 \pm 3.3$ eu). (c) Eyring plot comparing the 0.011 M mixed dimer experiment of part (a) and (b) (filled circles and squares) with data from a similar variable temperature study of a solution 0.16 M in **5** and 0.16 M in **8** (PhLi) (open circles and squares), showing that the rates are experimentally indistinguishable.

are within experimental error of the corresponding rates measured for pure **5** (Figure 13).

The quality of the simulations validates the assumptions that were made, i.e., that the exchanges of the three dimers largely involve unimolecular dissociations, without the participation of trimers or tetramers. This conclusion was also supported by a parallel experiment run at a 16-fold higher concentration.[15] Although the Eyring plots for this rate study showed more scatter than the one shown in Figure 15b, the principal rates (dissociation of **5D** and **15**) were within experimental error of each other (Figure 15c), ruling out bimolecular exchange processes observed for the dimer−monomer exchange for **1**.

The dimer dissociation rates follow the trends found in other chelated ArLi reagents. For example, the relative rates of dissociation of **8D**, **15**, and **5D** at −83 °C are calculated to be 540:17:1.9 from the activation parameters ($\Delta G^‡_{-83} = 8.6$, 9.9, and 10.7 kcal/mol). There is thus approximately 1 order of magnitude increase in kinetic stability of the dimer for each chelating CH_2CH_2OMe group, similar to the increase in monomer−dimer association (K_{MD}) values.

Carbon−Carbon Coupling in the Side Chain of 4 and 5. The information provided above provides strong circumstantial evidence that **4** and **5** are chelated. We have attempted to provide more direct evidence by measuring $^2J_{COC}$ and $^3J_{CCOC}$ in the side chain, in anticipation that the conformational changes of a chelated vs a nonchelated structure might result in diagnostic trends in these coupling constants. We prepared O−$^{13}CH_3$ labeled **4** and **5** and measured the 3-bond and 4-bond coupling in the lithium reagent and model compounds (Figure 16). The couplings in the various nonchelated (or largely nonchelated) models are essentially identical, and in each case there is significant change in the coupling on going to the organolithium reagent. There are also substantial chemical shift changes, especially of the benzylic carbon, which are also in part due to the conformational changes resulting from chelation. However, the strongly polarizing C−Li bond is the principal source of these changes, as shown by the fact that the methyl group of *o*-tolyllithium monomer (δ 30.1) moves downfield by 8.7 ppm from its position in toluene (δ 21.4). Thus the coupling constants also may reflect changes in electronic structure as much as changes in conformation. Although the changes in couplings support the conclusions reached from other experiments that **4** and **5** are chelated, they are probably not large enough to provide firm evidence on their own.

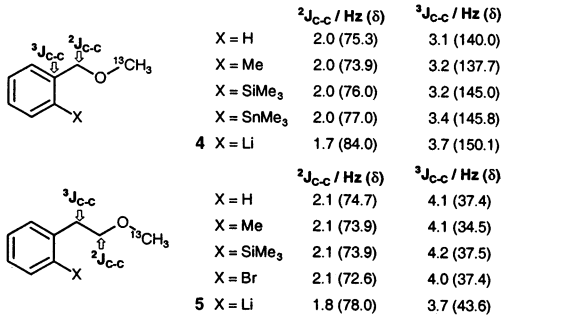

Figure 16. Carbon−carbon couplings and chemical shifts in $^{13}CH_3O$ **4**, **5** and model compounds in 3:2 THF/Et_2O at 11 °C.

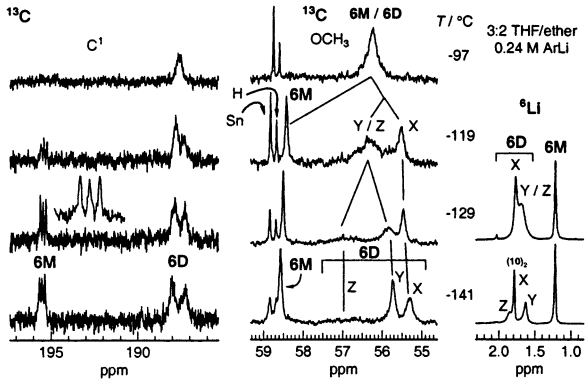

Figure 17. Variable-temperature ^{13}C and ^{6}Li NMR spectra of **6**. Shown are the C−Li carbons (left), the methoxy signals (center) and the ^{6}Li signals (M = monomer, D = dimer). The peaks marked "H" and "Sn" in the −119 °C spectrum are the OMe signals of the protonated product (3-methoxypropyl)benzene and trimethylstannyl precursor.

Seven-Membered Ring Ether Chelation−2-(3-Methoxypropyl)phenyllithium (6). We have also examined the potentially 7-ring chelated ether **6**. The ^{6}Li and ^{13}C NMR spectra at −141 °C show a monomer as a prominent species (ca. 34% of total at 0.24 M in 3:2 THF/Et_2O, $K_{MD} = 12$ M^{-1}). In the ^{6}Li NMR spectra three additional signals were present (Figure 17). These signals were assigned to dimers from analysis of variable concentration experiments,[15] and from the characteristic ^{13}C line shape and chemical shifts of the C−Li carbons (δ 187.5 and 188.0). Unfortunately, one variable-concentration experiment gave aggregation as high as 3.5, so more work would need to be done to conclusively rule out, for example, cyclic trimer structures for one or more of the three signals.

Dynamic Processes for 6. A variable-temperature ^{6}Li NMR experiment[15] showed that two of the dimers coalesced at −130 °C, the two remaining dimer signals at −120 °C, and finally the averaged dimers coalesced with the monomer at −100 °C ($\Delta G^{\ddagger}_{-107}$ = 8.8 kcal/mol).

Detailed assignment of the dimer signals of **6** was hampered by the low temperatures needed and their peculiar properties. We have labeled the three dimer signals **X**, **Y**, and **Z**, and the monomer signal **M** (Figure 17). At −141 °C the **Z**-MeO ^{13}C NMR signal as well as the **Z**-^{6}Li signals are substantially broader than the others. By −129 °C the signal for **Z**-MeO has sharpened a little, but has now begun to coalesce with the **Y**-OMe signal. The **Y** and **Z** signals are already coalesced in the ^{6}Li NMR spectrum because of the much smaller separation (13 Hz for ^{6}Li vs 120 Hz for ^{13}C) between the signals. This process causes no detectable change in the C−Li carbons. The **X** ^{13}C signal coalesces with **Y**/**Z** between −118 °C and −105 °C, and finally the averaged dimer signals coalesce with monomer between −105 and −96 °C. Presumably, the **X**, **Y**, and **Z** signals correspond to two or three of the chelation isomers **A**, **B**, and **C**.

The very low-temperature broadening of the **Z** signals suggests additional complications from a slowing of some conformational process of the methoxypropyl side chain (either chelate ring inversion, chelation/dechelation or configurational isomerization at tricoordinate oxygen) analogous to that detected for 2-diethylaminomethylphenyllithium at very low temperatures.[1h] In fact, the simplest explanation for the behavior in THF is that there are only two dimer structures, and that the complex low-temperature dynamic behavior is the result of conformational processes. This would fit well with the spectra seen in Et_2O solution,[15] where only two sets of signals (3:2 ratio) are seen in both the Li (δ 1.5 and 1.7) and ^{13}C NMR spectra (δ_{C-Li} 188.2, 186.8), which both appear to be dimers. The signals coalesce between −110 °C and −90 °C.

Although chemical shift arguments are inherently weak, the data in Figure 17 provide evidence that, like **2**, the dimers of **6** are chelated, whereas the monomer is not. Consider the chemical shifts of the MeO carbons: the various dimer signals are 1.5−4 ppm upfield of the signal of 3-(methoxypropyl)benzene (the protonation product) at δ 58.75, suggesting enforced proximity to the ring system, whereas that of the monomer (δ 58.57) is within 0.18 ppm, and within 0.34 ppm of the signal of the trimethylstannyl precursor (δ 58.91).

Interaction of 6 with TMEDA. The TMEDA titration is shown in Figure 18. As with **2** (Figure 6) it was necessary to measure the spectra below −140 °C to observe the individual species. Three new signals appear. The one at δ 1.6 can be assigned to the monomer−TMEDA complex since it coalesces with the THF-monomer signal above −140 °C. The downfield shift of 0.4 ppm is nearly identical to that observed for **2** and PhLi when they are converted to TMEDA complexes. The other two signals at δ 1.8 and 2.0 remain in a 1:1 ratio throughout the titration. We assign these to the two signals of an A-type dimer-TMEDA complex.

We have attempted to quantitate the interaction of **6** with TMEDA by simulation of the spectra of Figure 18a. It was necessary to do a DNMR simulation because of partial coalescence between **6M**·TMEDA and **6M** as well as between the **Y** and **Z** dimer signals (Figure 17). The results of the analysis

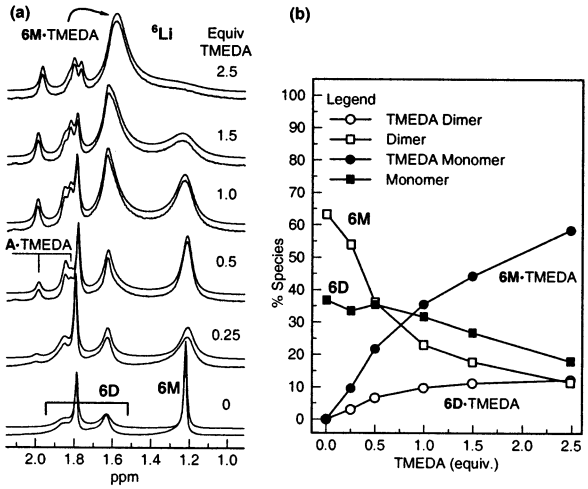

Figure 18. (a) ^{6}Li NMR spectra of a TMEDA titration experiment of 0.2 M [^{6}Li]**6** in 3:2 THF/Et_2O at −138 °C to −145 °C. The upper trace of each pair is a 7-spin DNMR simulation[11k] used to integrate the spectra. (b) Graphical presentation of the concentrations of the components of the equilibrium.

are presented in Figure 18b. As was observed in the more qualitative analysis done for **2**, TMEDA caused a modest level of dimer dissociation when complexed to **6**. This can be expressed in terms of two pairs of equilibrium constants. First the monomer−dimer association constants (t = TMEDA): $K_{MD-THF} = [D]/[M]^2 = 8 \pm 3\ M^{-1}$, $K_{MD-t} = [D{\cdot}t]/[M]\ [M{\cdot}t] = 2.4 \pm 0.3\ M^{-1}$. Second, the TMEDA-affinity of monomer and dimer: $K_{M-t} = [M{\cdot}t]/[M]\ [t] = 9.5 \pm 1.4\ M^{-1}$; $K_{D-t} = [D{\cdot}t]/[D]\ [t] = 3.0 \pm 0.6\ M^{-1}$. The TMEDA-complexed aryllithium is about one-third as aggregated, and the monomer has three times the TMEDA-affinity as does the dimer.

Interaction of 6 with PMDTA. The addition of PMDTA stoichiometrically converted all signals in the ^{6}Li and ^{13}C NMR spectra into signals of monomeric **6M**·PMDTA.[15] This is consistent with the behavior of all other ArLi compounds we have investigated that are significantly monomeric in THF.

Chelation and Aggregation. The data reported here demonstrate a broadly based qualitative (and in a few cases, quantitative) correlation between chelation and the kinetic stability and thermodynamic preference for dimers in amine and ether-chelated aryllithium reagents. Table 1 summarizes the thermodynamic and kinetic data we have collected. For two of the compounds, the 5-ring chelates **1**[1h] and **4**, no monomer was detected by NMR spectroscopy in THF-ether solutions, so only upper limits of K_{MD} can be obtained. For three compounds (**2**, **5**, and **6**), both monomer and dimer were observed and both thermodynamic and kinetic stability could be measured.

The free energy of dimerization increases by 3.2 kcal/mol on going from the model system with an ortho ethyl group to the 6-ring ether chelate **5** (increase in K_{MD} by almost 5 orders of magnitude), and by more than that for the 5-ring ether and amine chelates (**4** and **1**). Similarly, the activation energy for dissociation of monomers increase by 3 kcal/mol for **4**, 4 kcal/mol for **6** and 5 kcal/mol for **1** compared to the model. The sequence of dimer stabilities from the available K_{MD} values is: **1** ≥ **4** > **5** > **2** > **6** > **3**, **7**. A similar order is also found for the kinetic stability of those dimers for which DNMR techniques could be used to measure rates (Table 1). Here, we find that $\Delta G^{\ddagger}$ is in the order **1** > **5** ≥ **4** > **2** > **6** > **7**.

We have used the behavior with TMEDA and PMDTA as probes into the effect of chelation ring size and chelating group[11] on the structures of aryllithium reagents. TMEDA disturbs the monomer−dimer equilibrium in only a minor way (showing, e.g., about a factor of 3 preference for monomer over dimer in **2** and **6**) and so can be used to probe the nature of the chelation (**A**, **B**, or **C** structures, Scheme 2). Three of the structures which are known or are likely to have **A**-type dimers present (**1**, **2**, and **6**) readily complex with TMEDA to form **A**-type TMEDA complexed dimers, with a characteristic 1:1 ratio of two signals in the Li NMR spectra. The 5- and 6-ring oxygen chelates **4** and **5** do not detectably complex with TMEDA, and we conclude that these must have a strong preference for **B** and/or **C**-type dimers which cannot form bidentate complexes with TMEDA.

The behavior with PMDTA is particularly instructive. The observation that excess PMDTA converts **2** through **6** completely to monomers, whereas TMEDA[22d] only minimally increases the fraction of monomers, means that the PMDTA complexes must be *tridentate*. (PMDTA is a poorer *bidentate* ligand than TMEDA). In addition, it appears that, with the exception of **4**·PMDTA, chelation is broken in the monomer-PMDTA complexes. Thus, the fraction of such species formed provides a qualitative measure of the strength of chelation because simple steric effects of the ortho-substituent should be similar through the series. This analysis could be performed quantitatively for **5** (Scheme 4), which showed that the dimer was substantially stabilized by chelation, whereas the monomer was not. It could not be applied to **4**, because the PMDTA complex is chelated (chelating ligands for lithium also show idiosyncratic behavior in the lithium amides[22e]). The nonchelating model **7** as well as **2**, **3**, and **6** show >96% conversion to the monomeric complex with 1 equiv of PMDTA. Chelation effects are very evident for **5** and **4**, which were only partially converted to monomer at 1 equiv of PMDTA.[10] Compound **1** is most strongly affected, because it forms no detectable monomer on addition of PMDTA.[1h] We conclude that the sequence of chelation strength (ΔG_{Chel}) is: **1** ≫ **4** > **5** > **2**, **6**, **3**, **7**, basically in the same sequence as the kinetic and thermodynamic stability of the dimers.

The thermodynamics and dynamics of **15**, the mixed dimer between **5** and PhLi, also provide a clear-cut example of the close relationship between chelation and aggregation. The monomer−dimer association constants (K_{MD}) increase by about an order of magnitude on going from the PhLi homodimer, to the mixed dimer **15** (with one chelating group) and then to the homodimer of **5** (with two chelating groups). This although a nonchelating ortho alkyl substituent reduces K_{MD} by over 2 orders of magnitude (compare PhLi and **7**, Table 1).

The relationship between aggregation and chelation is strikingly illustrated by the behavior of **2**, where both monomer and dimer can be observed. The dimer is unambiguously and fully chelated, whereas the monomer is unchelated. Although the evidence is weaker, this also seems to be the case for **5** and **6**.

Compound **4** shows several kinds of anomalous behaviors, most notably the formation of an open dimer PMDTA complex[12c] **12** not detected for any other aryllithium investigated. Also interesting is the observation that the PMDTA complex of **4** is tridentate and chelated, representing a stable pentacoordinate lithium structure, albeit one with an unusually labile ligand. Apparently, the small chelation ring size and the small steric size of the methoxy chelating group allow higher coordination than is usually observed for organolithium species.

We have previously discussed possible origins of the strong correlation between aggregation and chelation in connection with **1**.[1h] This paper has provided a number of additional and more specific examples of the effect. One plausible explanation involves consideration of the smaller C−Li−X (X = solvent or chelating group) bite angle in a 5- or 6-ring chelate versus an externally solvated one, which could lead to less cancellation of the C−Li dipole by the Li−X dipoles, and thus a higher propensity for aggregation. The smaller bite angle would also result in less steric inhibition of dimerization. Some evidence for a more polar C−Li bond in 5-ring amine-chelated organolithiums than in nonchelated models was provided by the higher HMPA-affinity of chelated $Me_2(Me_2NCH_2)SiCHLiSPh$ versus the unchelated model $Me_3SiCHLiSPh$. Unfortunately, no difference in HMPA affinity was seen between the 5-ring ether-chelated compound, $Me_2(MeOCH_2)SiCHLiSPh$, and the model,[1h] so this test does not support the bite-angle hypothesis for the ethers. We do not currently have a convincing and experimentally testable rationale for the correlation between aggregation and chelation.

Summary

For these systems amine chelation is strong in five-membered rings (**1**), competitive with THF solvent in six-membered rings (**2**), and absent in seven-membered rings (**3**). Ether chelation is of intermediate strength in both five- and six-membered rings, with the five-membered ring chelate **4** slightly more robust by most criteria.[10] The 7-ring ether **6** appears to be weakly chelated. There is a strong qualitative correlation between the strength of the chelation, as judged by the effect of PMDTA, and the strength of the aggregation, as judged by response to polar cosolvents, magnitude of monomer−dimer association constant K_{MD}, and rates of monomer−dimer equilibration.

Experimental Section

General. All reactions requiring a dry atmosphere were performed in glassware flame-dried or dried overnight in a 110 °C oven, sealed with septa and flushed with dry N_2. Tetrahydrofuran (THF) and Et_2O were freshly distilled from sodium benzophenone ketyl under N_2. Me_2O was purified by condensing several mL in a graduated conical flask at −78 °C from a pressurized gas cylinder, adding a small portion (0.5 mL) of *n*-BuLi and distilling the dry Me_2O via cannula into the desired vessel at −78 °C. *N,N,N′,N′*-Tetramethylethylenediamine (TMEDA), *N,N,N′,N″,N″*-pentamethyldiethylenetriamine (PMDTA) and hexamethylphosphoric triamide (HMPA) were distilled from CaH_2 under reduced pressure (if necessary) and stored over 4 Å molecular sieves under N_2. Common lithium reagents were handled with septum and syringe-based techniques and titrated against dry *n*-propanol in THF using 1,10-phenanthroline as indicator.[28] [^{6}Li]BuLi[16c] and [^{6}Li]EtLi[22f] were prepared by literature methods.

Low-Temperature NMR Spectroscopy. All low-temperature NMR spectra were acquired on Bruker AM-360 or AVANCE spectrometers using a 10 mm broadband probe at the following frequencies: 360.148 MHz (^{1}H), 90.556 MHz (^{13}C), 52.984 MHz (^{6}Li), 139.905 MHz (^{7}Li) and 145.785 MHz (^{31}P). All spectra were taken with the spectrometer unlocked. ^{13}C NMR spectra were referenced internally to the C−O carbon of THF (δ 67.96), Et_2O (δ 66.57) or Me_2O (δ 60.25). Lorentzian multiplication (LB) of 2−3 Hz was applied to ^{13}C spectra. ^{6}Li and ^{7}Li

(28) Watson, S. C.; Eastham, J. F. *J. Organomet. Chem.* **1967**, *9*, 165−168.

spectra were referenced externally to 0.3 M LiCl in MeOH (δ 0.00) or internally to $Li^+(HMPA)_4$ (δ −0.40). ^{31}P NMR spectra were referenced externally to 1.0 M PPh_3 in THF (δ −6.00) or internally to free HMPA (δ 26.40). Probe temperatures were measured externally by ejecting the sample and inserting a thermocouple into the probe or internally with the ^{13}C chemical shift thermometer $(Me_3Si)_3CH$.[1j]

General Procedure for NMR Spectroscopy of Organolithium Reagents. Samples of organolithium reagents (0.5 mmol in 3 mL of solvent) were prepared in thin-walled 10 mm NMR tubes that were oven-dried overnight, fitted with 9 mm i.d. septa, and flushed with N_2. Silicon grease was applied to the interface between the tube and the septa before securing with Parafilm for a better seal, as well as to the top of the septa to seal needle punctures. Samples were stored at −78 °C. After initial adjustment of the shim values the probe was cooled to −120 °C, the sample was inserted and the sample was shimmed on the ^{13}C FID of one of the solvent peaks (THF, Et_2O or Me_2O). Spectra of NMR active nuclei which usually included ^{13}C, ^6Li, ^7Li, and ^{31}P were measured. At this point, a cosolvent titration, variable temperature (VT) or variable concentration experiment could be performed. In the case of a titration experiment, for each addition the sample was ejected, placed in a −78 °C bath, the silicon grease was removed from the top of the septum, a desired amount of cosolvent was added, silicon grease was reapplied to the top of the septum and the desired NMR spectra were measured. Probe temperatures were measured internally with the ^{13}C chemical shift thermometer $(Me_3Si)_3CH$[1j] or externally by ejecting the sample and inserting a thermocouple into the probe.

The use of 10 mm NMR tubes provided a real advantage over 5 mm tubes because of the approximate 3-fold signal-to-noise enhancement with more sample in the magnetic field, more accurate additions of cosolvents, and minimal sample warming when transferring tubes from the −78 °C bath to the NMR probe.

General Procedures for Preparation of Aryllithium Reagents for NMR Spectroscopic Study. Crystallization from Diethyl or Dimethyl Ether. The precursor aryltrimethylstannane was added to a dried and N_2-flushed 10 mm NMR tube. The tube was cooled to −78 °C and 1 mL of Me_2O (or Et_2O, when noted) was condensed into it. Me_2O was an ideal solvent for this crystallization method, because the lithium/tin exchange was relatively fast and the aryllithium reagents were usually not very soluble in pure Me_2O. The NMR tube was temporarily removed from the −78 °C bath, warmed slightly, and shaken to dissolve the arylstannane. The addition of 1.0 equiv of *n*-Bu^6Li to the NMR tube gave a homogeneous yellow solution. The NMR tube was stored overnight at −78 °C, while the aryllithium reagent crystallized from solution. The yellow supernatant was removed by cannula transfer and the crystals were washed with Et_2O (2 × 0.5 mL) at −78 °C. The crystals were dissolved in a combination of THF and Et_2O, by warming the solvent mixture, if necessary to room temperature, and vigorously shaking the NMR tube, to give a clear, colorless solution of aryllithium reagent with concentrations ranging from 0.08 to 0.16 M. The NMR tube was returned to the −78 °C bath, and Me_2O was added if needed. The sample was ready for NMR investigation.

Direct Preparation of Sample in 3:2 THF/Et_2O. The aryllithium precursor aryltrimethylstannane (0.50 mmol), 1.8 mL of THF and 1.2 mL of Et_2O were added to a dried and N_2-flushed 10 mm NMR tube. After cooling to −78 °C, 0.63 mL of 0.79 M *n*-Bu^6Li (or Et^6Li) in hexanes (0.50 mmol, 1.00 equiv) was added to give a yellow solution with an initial aryllithium concentration of 0.14 M. The sample was stored for 30 min at −20 °C to ensure the lithium−tin exchange was complete before beginning the NMR experiment.

Quantitation of Arylithium Reagents. The concentrations of aryllithium solutions were determined by the following methods. (1) In some cases when the lithium reagent was prepared by Li/Sn exchange, quantitative transmetalation was assumed. (2) Quenching of the aryllithium reagent with Me_2S_2, Me_3SiCl or PhCHO followed by quantitation of the sulfide, silane or benzyl alcohol by ^1H NMR spectroscopy and/or GC analysis were used to determine the yield and demonstrate the location of the carbanion during the experiment. For example, the NMR sample was quenched with 1.5 equiv of Me_3SiCl to give the corresponding arylsilane, diluted with 20 mL of 1:1 ether/hexanes, washed with 100 mL of distilled water or saturated Na_2CO_3 and 100 mL of brine. The organic fraction was dried over $MgSO_4$, filtered and concentrated in vacuo. The yield of the arylsilane was determined by ^1H NMR integration against pentachloroethane as a standard. (3) HMPA has been shown to bind aryllithium reagents in a stoichiometric fashion in THF and Et_2O solutions,[1h] thus initial addition of HMPA was assumed to complex aryllithium stoichiometrically. Integration of the complexed versus uncomplexed aryllithium species in the ^6Li NMR spectrum allowed the solution concentration to be determined. Stoichiometric HMPA complexation was confirmed by examining the ^{31}P NMR spectrum for free HMPA.

Dynamic NMR Simulation. Many of the variable temperature NMR spectra were simulated to determine rate constants, activation parameters and/or peak areas. These simulations were performed with the computer program WINDNMR,[1k] using one of the standard exchange matrixes (random exchange of singlets) or custom setups for more complex situations.

Acknowledgment. We thank NSF for financial support (CHE-0074657) and funding for instrumentation (NSF CHE-9709065, CHE-9304546). Prof. Gideon Fraenkel provided assistance with setting up exchange matrixes for the DNMR simulation of the C-Li exchange of **4**.

Supporting Information Available: Experimental procedures for the preparation of compounds and NMR samples, ^6Li, ^{13}C, and ^{31}P NMR spectra of NMR experiments not presented in the main body of this paper. This material is available free of charge via the Internet at http://pubs.acs.org.

JA028301R